Revealing the Biochemical and Genetic Basis of Color Variation in a Polymorphic Lizard

Claire A. McLean,*[,1,2] Adrian Lutz,[1,3] Katrina J. Rankin,[1] Devi Stuart-Fox,[†,1] and Adnan Moussalli[†,2]

[1]School of BioSciences, The University of Melbourne, Parkville, VIC, Australia

[2]Sciences Department, Museums Victoria, Carlton Gardens, VIC, Australia

[3]Metabolomics Australia, The University of Melbourne, Parkville, VIC, Australia

[†]These authors contributed equally to this work.

***Corresponding author:** E-mail: mcleanca@unimelb.edu.au.

Associate editor: Yoko Satta

Abstract

Determining the mechanistic and genetic basis of animal coloration is essential to understand the costs and constraints on color production, and the evolution and maintenance of phenotypic variation. However, genes underlying structural color and widespread pigment classes apart from melanin remain largely uncharacterized, in part due to restricted taxonomic focus. We combined liquid chromatography-mass spectrometry and RNA-seq gene expression analyses to characterize the pigments and genes associated with skin color in the polymorphic lizard, *Ctenophorus decresii*. Throat coloration in male *C. decresii* may be a combination of orange, yellow, grey, or ultra-violet blue. We confirmed the presence of two biochemically different pigment classes, pteridines (self-synthesized) and carotenoids (acquired through the diet), in all skin colors. Orange skin had the highest levels of pteridine pigments while yellow skin tended to have higher levels of carotenoids, of which the vitamin A precursors β-carotene and β-cryptoxanthin have not been previously confirmed in reptiles. These results were confirmed by gene expression analyses, which detected 489 genes differentially expressed between the skin colors, including genes associated with pteridine production, provitamin A carotenoid metabolism, iridophore-specific synthesis, melanin synthesis, and steroid hormone pathways. For the majority of these 489 genes, however, our study reveals a new association with color production in vertebrates. These data represent a significant contribution to understanding the genetic basis of color variation in vertebrates and a rich resource for further studies.

Key words: **carotenoid, color polymorphism, liquid chromatography-mass spectrometry, pteridine, RNA-seq.**

Introduction

While our understanding of color production mechanisms in animals is advancing, less is known about the molecular basis of these processes and, in particular, the genetics of color variation within species (Hubbard et al. 2010; Olsson et al. 2013). This is essential to understand the costs and constraints on color expression, and consequently, the evolution and maintenance of phenotypic variation. The majority of research into the genetics of color variation in wild populations has focused on melanin-based traits (Hubbard et al. 2010). Pathways and candidate genes for melanin-based color traits are well-understood (Hoekstra 2006; Braasch et al. 2007; Poelstra et al. 2015; Küpper et al. 2016; Schweizer et al. 2016; Toews et al. 2016; Tuttle et al. 2016), relative to those controlling production or transport of other widespread pigment classes such as pteridines and carotenoids (but see Diepeveen and Salzburger 2001; Braasch et al. 2007; Salzburger et al. 2007; von Lintig 2010; Walsh et al. 2011; Lopes et al. 2016; Mundy et al. 2016). Furthermore, the genetic basis of structural coloration, in particular genes controlling the specific arrangement of structural components such as guanine, collagen and keratin, remains largely unknown. In part, this is because research has focused on a handful of model systems with specific mechanisms of color production. For example, mammals and birds use pigments to color dead, keratinized tissue (hair, fur, feathers, and beaks), whereas poikilothermic vertebrates (nonavian reptiles, fish, and amphibians) use a layered pigment cell system comprising multiple chromatophore types to produce a plethora of colors within the dermal layer of the skin. Despite their potential to broaden our understanding of the genetics of color variation, poikilothermic (lower) vertebrates, particularly reptiles, remain poorly studied in this regard (Olsson et al. 2013).

In reptiles, color is produced by the interaction between chromatophore cells and structural components (e.g., collagen and connective tissue) in the dermis. There are three chromatophore cells types: melanophores containing melanin pigments, iridophores containing light scattering and reflecting guanine crystals, and xanthophores containing carotenoid and/or pteridine pigments (reviewed in Grether et al. 2004; Olsson et al. 2013). Melanin pigments are responsible for brown-black coloration, with darker skin having higher concentrations of melanin. Conversely, blue is

Article

primarily a structural color produced by light scattering off the integument and platelets in the iridophores (Bagnara et al. 2007); however, the concentration of melanin can also significantly contribute to the intensity of ultra-violet and blue coloration (Morrison et al. 1995; Macedonia et al. 2000). Finally, yellow-red coloration is produced by carotenoid and/or pteridine pigments in the xanthophores, which absorb short wavelengths of light (violet-blue), allowing long wavelengths (yellow-red) to pass through and be reflected by the iridophores (Morrison et al. 1995; Macedonia et al. 2000).

Carotenoids must be obtained through the diet (McGraw 2006) while pteridines are synthesized in the body from purine molecules (Ziegler 2003; Braasch et al. 2007), and this variation in origin may inflict differing constraints on pigment production and the function of yellow-red signaling traits. One or both pigment types may be present within a species; however, previous studies have been limited in their ability to identify the specific metabolites involved. Often they have only confirmed the presence of either carotenoids (lipid soluble; Fitze et al. 2009) or pteridines (not lipid soluble; Morrison et al. 1995; Weiss et al. 2012) or a combination of both (Macedonia et al. 2000; Olsson et al. 2008; Haisten et al. 2015; Merkling et al. 2015), and made predictions about the likely metabolites within each of those classes. Identifying the specific metabolites, and their relative concentrations, is essential to understand the biochemical links between color expression and other cellular processes, which in turn provides insight into mechanisms maintaining color signal honesty (Hill and Johnson 2012). For example, some dietary carotenoids (α-carotene, β-carotene, γ-carotene, and β-cryptoxanthin) serve as precursors (i.e., provitamins) for vitamin A (retinol; von Lintig 2010; Hill and Johnson 2012) which regulates multiple cellular processes, including immune function, leading to the prediction that carotenoids may serve as an honest signal of individual quality. Despite this, provitamin A carotenoids have yet to be confirmed in reptiles.

Males of the Australian tawny dragon lizard, *Ctenophorus decresii*, are brightly colored and exhibit variation in coloration both within and among populations (Houston and Hutchinson 1998; McLean et al. 2013). There are two genetically and phenotypically distinct lineages within the species which differ most notably in male throat coloration (McLean et al. 2013 2014b). "Southern" males have blue throats which also reflect ultra-violet (UV) wavelengths of light (McLean et al. 2013 2014a), which *C. decresii* is able to perceive (as confirmed by analysis of retina transcriptomes; Yewers et al. 2015), while "northern" males are polymorphic with orange, yellow, orange-yellow (orange central patch surrounded by yellow), or grey throated males co-occurring within populations (fig. 1; McLean et al. 2013). Males prominently display their throats during encounters with rivals and mates (Gibbons 1979) and color morphs differ in a number of behavioral and physiological traits (Yewers et al. 2016). Furthermore, captive breeding and mark-recapture studies have confirmed that the discrete throat color morph is fixed at sexual maturity and is not size or condition dependent (Teasdale et al. 2013; Rankin and Stuart-Fox 2015). The presence or absence of orange and yellow throat coloration is most likely governed by two autosomal loci (Rankin et al. 2016), but the total area of orange or yellow on the throat within and between color morphs is a highly heritable quantitative trait (Rankin et al. 2016), which indicates that many genes are likely to be involved in color expression in this species.

We used highly sensitive liquid chromatography-mass spectrometry (LC-MS) to identify specific pigments and compare their concentrations within and among *C. decresii* skin samples of different colors. Additionally, we sequenced skin transcriptomes (along with a number of other tissue types) to identify genes which were differentially expressed among skin colors. All skin colors (blue, grey, cream, orange, and yellow) contain the three pigment cell types that typically comprise the dermal chromatophore unit in reptiles: melanophores, iridophores, and xanthophores (Lewis A, Rankin K, Pask A, Stuart-Fox D, unpublished data; supplementary fig. S1, Supplementary Material online). By combining targeted metabolomic and transcriptomic analyses we were able to detect genes potentially associated with chromatophore cells and/or pigment production, transport, and storage. We highlight these candidate color genes for further study of the genetic basis of both discrete and continuous color variation in vertebrates.

Results and Discussion

Pteridine and Carotenoid Pigments Generate Yellow and Orange Skin Coloration

Yellow and orange skin coloration of *C. decresii* is produced by a combination of both carotenoid and pteridine pigments. Using LC-MS, we identified six carotenoids (astaxanthin, 3′-dehydrolutein, lutein, and/or zeaxanthin, canthaxanthin, β-cryptoxanthin, β-carotene) and seven pteridines (xanthopterin, 6-biopterin, pterin, isoxanthopterin, pterine-6-carboxylic acid, drosopterin, and sepiapterin). Notably, these included β-carotene and β-cryptoxanthin, the presence of which has not previously been verified in reptiles due to limitations of methods employed (e.g., the highly lipophilic β-carotene often fails to elute in chromatography; Haisten et al. 2015). Our identification of these metabolites in *C. decresii* is significant given that carotenoid based coloration is often hypothesized to act as an honest signal of condition, partly due to the contribution of carotenoids to immune function; however, this only applies to the few carotenoids (including β-carotene and β-cryptoxanthin) which convert to the antioxidant vitamin A (Olson and Owens 1998; Svensson and Wong 2011).

Relative concentrations of individual metabolites differed significantly between skin colors (table 1; fig. 2). Yellow skin tended to have the highest levels of carotenoid pigments (fig. 2). The levels of the yellow pigments 3′-dehydrolutein ($P = 0.003$), lutein/zeaxanthin ($P < 0.001$), and β-cryptoxanthin ($P = 0.011$), and the orange-red pigment canthaxanthin ($P = 0.001$) were significantly higher in yellow skin than in grey skin (fig. 2; supplementary table S1, Supplementary Material online). Orange skin also had higher levels of 3′-dehydrolutein ($P = 0.029$) and lutein/zeaxanthin ($P = 0.010$) than grey skin (fig. 2; supplementary table S1, Supplementary Material online). Additionally, orange skin had the highest

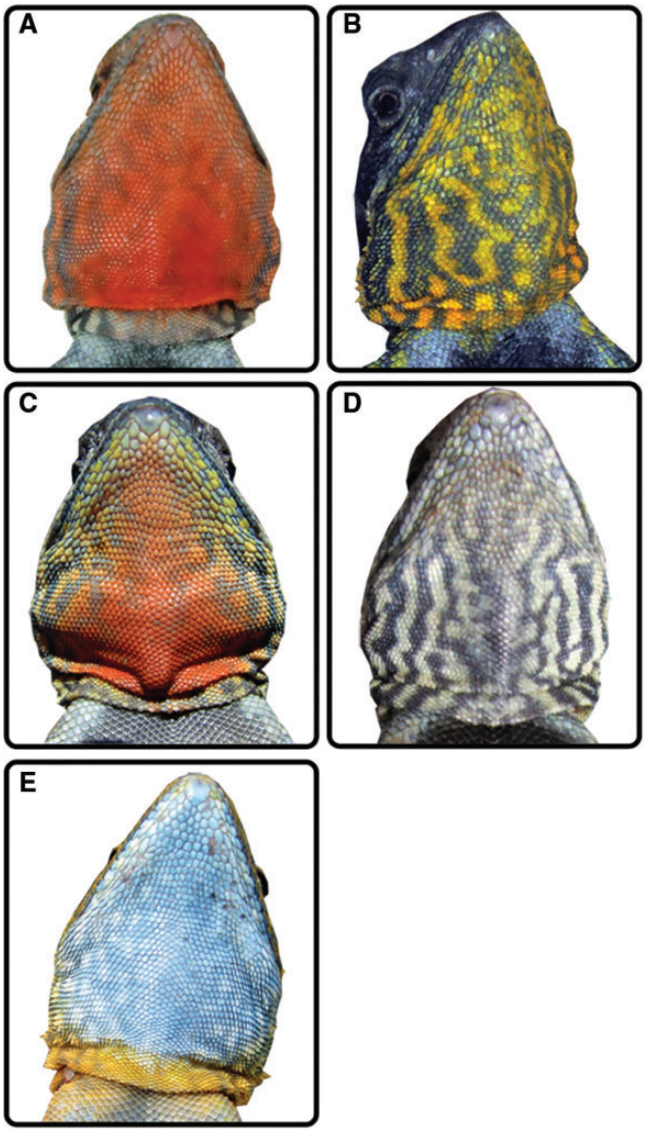

Fig. 1. Male throat color variation in the tawny dragon lizard, *Ctenophorus decresii*. Northern lineage males are polymorphic, with (**A**) orange, (**B**)* yellow, (**C**) orange-yellow, and (**D**) grey throats, while Southern lineage males are monomorphic with (**E**) ultra-violet blue throats.

levels of all pteridine pigments. These included four colorless pteridines (6-biopterin, pterin, isoxanthopterin, and pterine-6-carboxylic acid; all $P < 0.05$), which are unlikely to contribute to skin color, but may act as precursors to colored pigments (fig. 3), as well as the yellow pigment xanthopterin (orange vs. grey: $P = 0.001$; orange vs. yellow: $P = 0.007$) and the red pigment drosopterin (orange vs. grey: $P = 0.023$; fig. 2; supplementary table S2, Supplementary Material online). Therefore, yellow and orange skin primarily differs in the relative concentrations of yellow carotenoids and colored pteridines. This pattern appears to be consistent with other reptile species (e.g., Jamaican anoles, *Anolis sagrei*, day geckos, and *Uta stansburiana*; Macedonia et al. 2000; Steffen et al. 2010; Saenko et al. 2013; Haisten et al. 2015), including the congeneric and polymorphic *Ctenophorus pictus* (Olsson et al. 2008); although in these species the relative concentrations of individual metabolites within and among skin colors and/or the specific pteridine or carotenoid pigments have not been identified.

Gene Expression Differs between Skin Colors

A total of 489 genes were differentially expressed between at least two skin colors (supplementary table S3, Supplementary Material online), indicating genetic differences underlying color production in *C. decresii*. Of these, 67 genes appear to have skin specific function as they were also more highly expressed in skin than in nonskin tissue (supplementary table S3, Supplementary Material online). The relatively small number of genes specific to a given skin color is expected given that all skin colors contain the same three pigment cell types (melanophores, iridophores, and xanthophores) that comprise the dermal chromatophore unit (Lewis A, Rankin K, Pask A, Stuart-Fox D, unpublished data; supplementary fig. S1, Supplementary Material online). Twenty-six of the 489 differentially expressed genes showed significantly higher or lower expression in blue skin relative to all other skin colors, while 14 were similarly unique to yellow skin. These results were visualized by principle component analyses of gene expression data, which revealed strong clustering of skin colors with the greatest separation between yellow and blue skin samples (fig. 4). We do, however, interpret this cautiously given that yellow and blue skin had the fewest samples and blue skin was from only southern individuals, and could therefore reflect gene expression differences between the lineages.

Pteridine Synthesis

The expression of individual genes involved in pteridine synthesis pathways did not differ significantly between skin colors (fig. 3); however, when considering the pteridine synthesis pathway as a whole using gene set enrichment analysis (GSEA), the pteridine gene set was upregulated in orange (FDR = 0.038) and yellow (FDR = 0.054) skin relative to blue skin. GSEA did not reveal differences between orange, yellow and grey skin, which was unexpected given that orange skin had higher levels of all pteridine pigments (fig. 2). Therefore, the timing of sampling may be important for detecting differential expression of specific genes or pathways among some skin colors. For this study, skin was sampled from sexually mature males; however, gene expression will vary across developmental stages, and thus skin may need to be sampled from juvenile lizards at the onset of adult coloration, or from developing scale buds.

Given that pteridine pigments are synthesized *de novo* from purine molecules, we also searched gene annotation terms for the keyword "purine". We found that 65 of the genes differentially expressed between skin colors were associated with purine metabolism, transport, or binding (supplementary table S3, Supplementary Material online). Purine molecules are not specifically associated with pteridine synthesis; for example, purines are also the precursors to guanine crystals in iridophores (Higdon et al. 2013), and none of these 65 purine-related genes showed expression patterns uniquely associated with orange skin. However, *carns1*, *mcm6*, *myh7*, and *nt5c1a* had higher expression levels in orange and blue

Table 1. Comparison of Carotenoid and Pteridine Pigment Responses in Orange ($N = 7$), Yellow ($N = 7$), and Grey ($N = 7$) Skin Samples

	Pigment	Color Produced	SS	F_{df}	P
Carotenoid	Astaxanthin	Red	0.128	$0.039_{2,\ 18}$	0.962
	3′-Dehydrolutein	Yellow	62.67	$8.057_{2,\ 18}$	*0.003*
	Lutein/Zeaxanthin	Yellow	7.948	$11.75_{2,\ 18}$	5.4×10^{-4}
	Canthaxanthin	Orange-Red	57.51	$9.663_{2,\ 18}$	*0.001*
	β-Cryptoxanthin	Yellow	2.621	$5.482_{2,\ 18}$	*0.014*
	β-Carotene	Orange-Red	1.690	$0.138_{2,\ 18}$	0.872
Pteridine	Xanthopterin	Yellow	4.070	$10.48_{2,\ 18}$	*0.001*
	6-Biopterin	Colorless/UV	2.805	$18.70_{2,\ 18}$	4.0×10^{-5}
	Pterin	Colorless/UV	4.605	$12.24_{2,\ 18}$	4.0×10^{-4}
	Isoxanthopterin	Colorless/UV	1.427	$3.454_{2,\ 18}$	0.054
	Pterine-6-Carboxylic Acid	Colorless/UV	3.473	$6.800_{2,\ 18}$	*0.006*
	Drosopterin	Orange-Red	38.36	$4.405_{2,\ 18}$	*0.028*
	Sepiapterin	Yellow	21.59	$2.368_{2,\ 18}$	0.122

Statistically significant *P*-values are italicized.
SS, sum of squares; df, degrees of freedom.

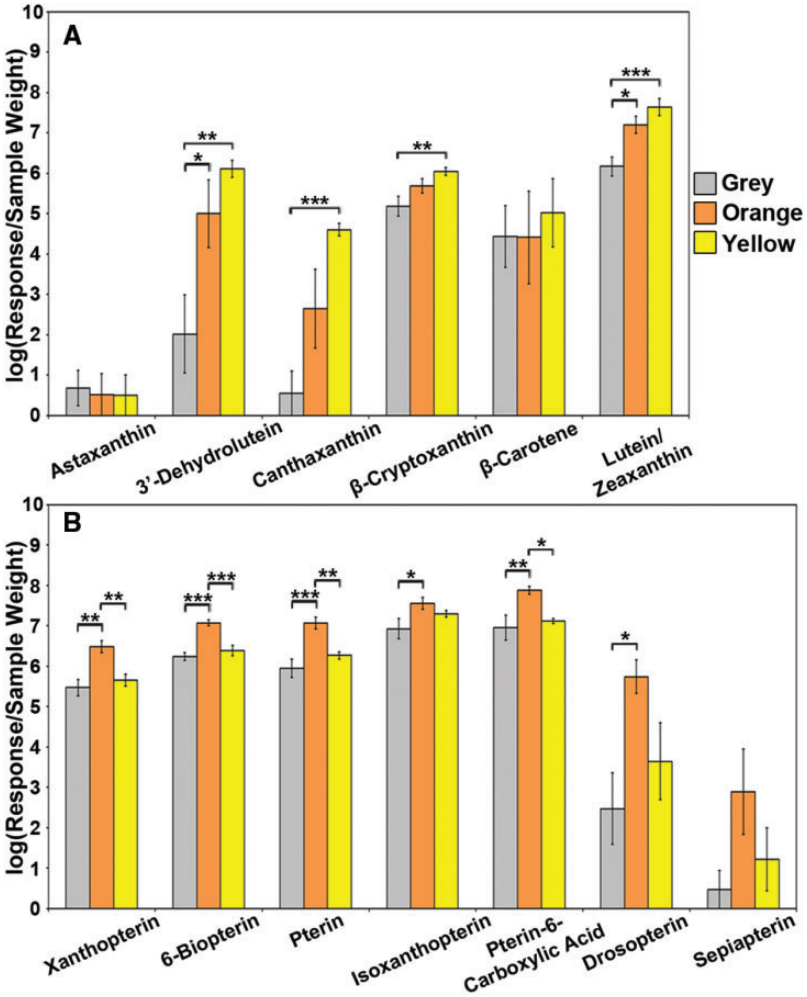

Fig. 2. Pigment levels differ among *C. decresii* skin of different colors. Mean ± SE (**A**) carotenoid and (**B**) pteridine pigment levels in grey, orange and yellow skin. Brackets indicate significant pairwise differences between skin colors: $^*P < 0.05$, $^{**}P < 0.01$, $^{***}P < 0.001$.

skin relative to yellow or grey skin. Furthermore, the expression levels of *ak5*, *gne* and *itm2c* were higher in both yellow and orange skin when compared to grey and blue skin (table 2; supplementary table S3, Supplementary Material online). Therefore, these genes may play important roles in generating skin color.

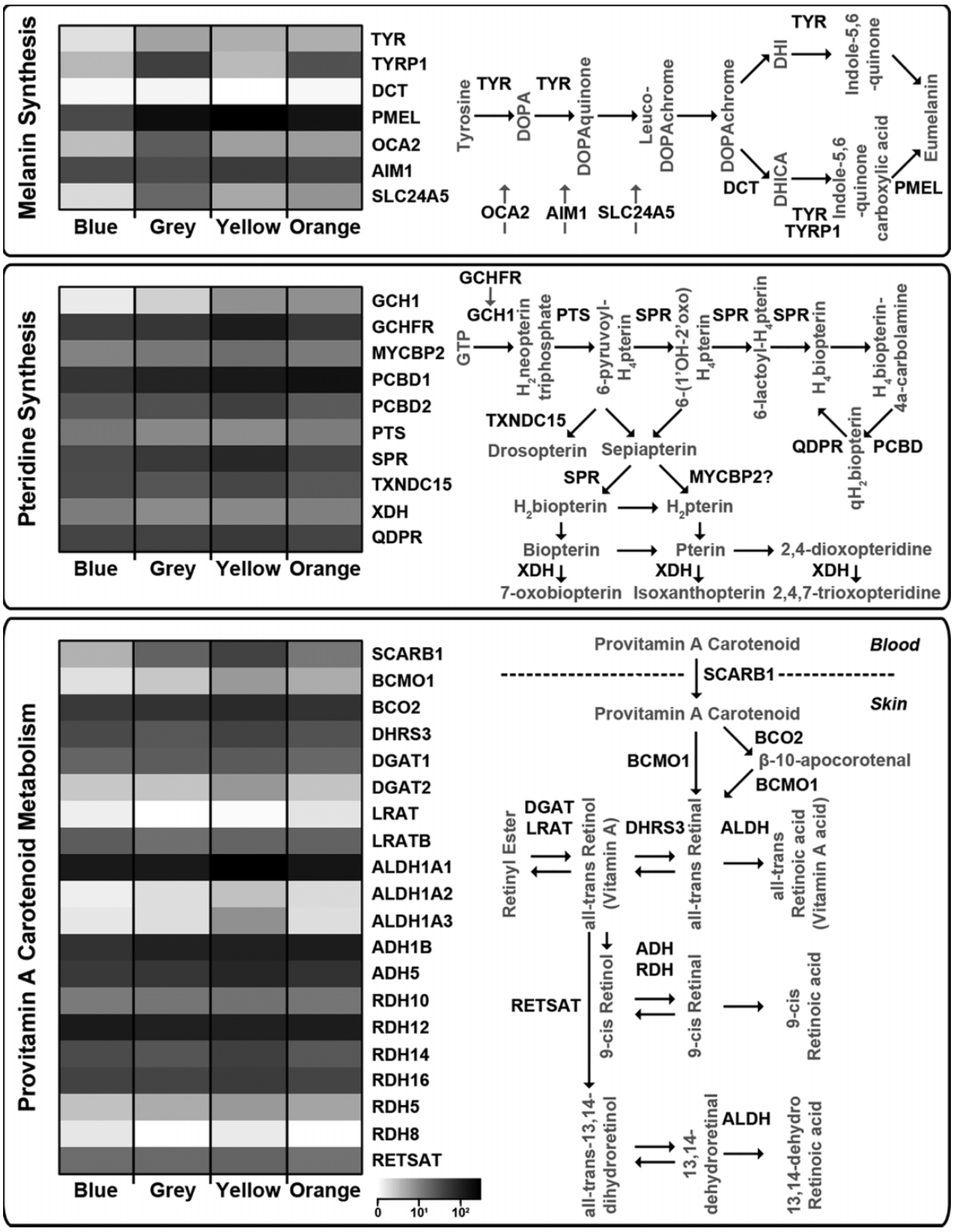

Fig. 3. Relative expression of pigment pathway genes. Heatmaps showing mean expression levels of the genes previously identified as involved in melanin and pteridine synthesis pathways (Braasch et al. 2007), and provitamin A carotenoid metabolism (Waagmeester et al. 2009) in blue ($N = 3$), grey ($N = 4$), yellow ($N = 2$), and orange ($N = 4$) *C. decresii* skin samples. Mean expression levels are log transformed for visualization.

Carotenoid Transport, Storage, and Metabolism

Unlike pteridine and melanin pigments which are synthesized in the body, carotenoids occur naturally in plants and must be obtained through the diet. Consequently, any genes associated with carotenoid-based coloration will be those involved in pigment transport, storage and/or metabolism (Diepeveen and Salzburger 2001; Salzburger et al. 2007; von Lintig 2010; Walsh et al. 2011). We have limited knowledge of

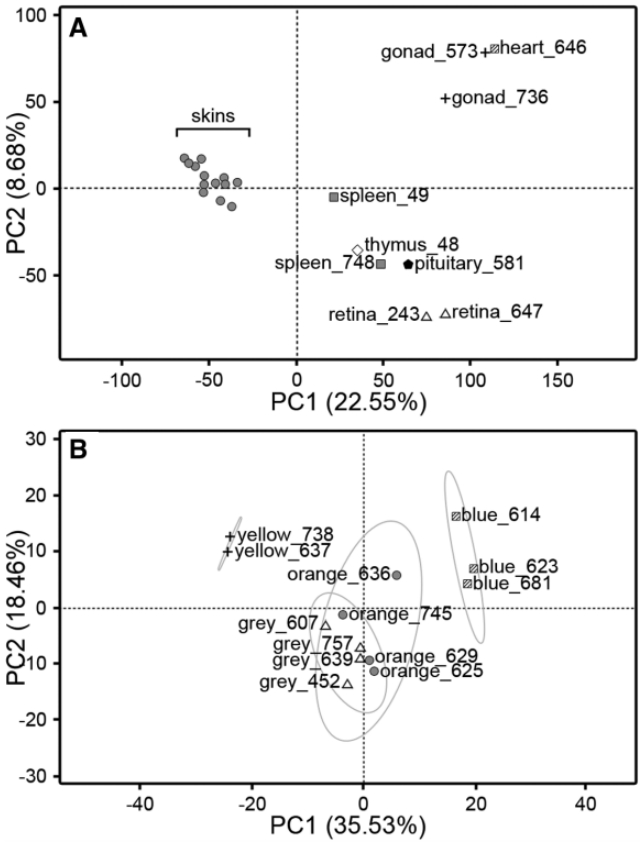

Fig. 4. Principle component analyses showing separation of samples based on gene expression estimates. Panel A shows separation of tissue types based on the full gene dataset while panel B shows clustering of skin colors based on the 489 genes which were differentially expressed between skin colors.

the genetics of carotenoid-based coloration as there have been only a few studies of carotenoid metabolism pathways, all of which have focused on the conversion of carotenoids (in particular, β-carotene) to vitamin A (reviewed in Eroglu and Harrison 2013). We found that three genes involved in provitamin A carotenoid metabolism (fig. 3) were differentially expressed between *C. decresii* skin colors: *aldh1a3*, *bcmo1* and *scarb1* (fig. 3; table 2; Eroglu and Harrison 2013). All three genes showed the highest expression levels in yellow skin (table 2; supplementary table S3, Supplementary Material online), and GSEA further revealed that the provitamin A carotenoid metabolism pathway was significantly enriched in yellow skin, relative to all other skin colors (all FDR < 0.05). Thus, the gene expression results corroborate those of the metabolomic analysis showing that carotenoid levels are highest in yellow skin (fig. 2).

Much less is known about genes associated with nonprovitamin A carotenoids, which also differed in relative concentration among skin colors of *C. decresii* (fig. 2). However, we searched for genes which showed similar expression patterns to those revealed by the metabolomic analyses, with higher levels in yellow and orange skin relative to grey skin. One such gene was *sepp1b* (orange vs. grey: FDR = 0.023, yellow vs. grey: FDR = 0.055; table 2), which is responsible for the transport and storage of selenium, which inhibits carotenoid production in plants (Sams et al. 2011) and like vitamin A, acts as an antioxidant. Therefore, we hypothesize that *sepp1b* may also be involved in the transport and storage of carotenoids, or alternatively selenium may be associated with yellow and orange color production in *C. decresii*.

Iridophore Cells

A previous study of differential gene expression in chromatophore cells of the zebrafish, *Danio rerio*, identified genes specifically enriched in iridophores (Higdon et al. 2013). We found that ten of these genes were also differentially expressed between skin colors of *C. decresii* (supplementary table S3, Supplementary Material online). Yellow skin had the highest expression (though not significantly higher for all pairwise comparisons) of *adamts13*, *anxa1*, *bpi*, *phyhd1*, *sesn1*, and *tmem179b*, and the lowest expression of *eno3* (table 2). While blue skin had the highest expression of *gnat2* and *pald1* and the lowest expression of *fhl2* (table 2). Differential expression of iridophore associated genes in yellow and blue skin supports our understanding of the role of these cells in color production in reptiles, with iridophores known to contribute to the generation of yellow-orange coloration (Macedonia et al. 2000; Steffen and McGraw 2009) and particularly structural UV-blue coloration (Bagnara et al. 2007).

Melanophore Cells and Melanin Synthesis

Our expectation was that melanin concentration would be highest in grey skin. Furthermore, investigation of *C. decresii* skin structure using transmission electron microscopy revealed that grey skin has a higher proportion of melanophores than either orange or yellow skin (Lewis A, Rankin K, Pask A, Stuart-Fox D, unpublished data). Melanin can also significantly contribute to the generation of blue and UV coloration by absorbing longer wavelengths of light not scattered or reflected by overlying iridophores. For example, both grey and blue skin of the fence lizard, *Sceloporus undulatus erythrocheilus*, contain approximately four times as many melanophores as yellow or orange skin (Morrison et al. 1995). We found that all skin colors expressed the genes previously identified as involved in the synthesis of eumelanin in vertebrates (fig. 3; Braasch et al. 2007), with the exception of *dct* (also known as *tyrp2*), which had very low expression levels in all samples and was only consistently expressed in grey skin. Three additional genes involved in eumelanin synthesis: *tyrp1*, *oca2*, and *slc24a5*, were differentially expressed between skin colors, with grey skin having significantly higher expression than either blue or yellow skin (fig. 3; table 2; supplementary table S3, Supplementary Material online). These patterns suggest that, as expected, melanin concentration is highest in grey skin and *dct*, *tyrp1*, *oca2*, and *slc24a5* appear to be the important rate limiting genes in the melanin production pathway (Lamason et al. 2005; Alonso et al. 2008).

An additional 12 genes which were differentially expressed between skin colors have been previously identified as enriched in *D. rerio* melanophore cells (Higdon et al. 2013) and/or have annotation terms including melanin or melanogenesis (supplementary table S3, Supplementary Material online).

Table 2. Differentially Expressed Genes with Previous Links to Color Production and Exhibiting Expected Patterns among Skin Colors

Gene name	Full name	Previous link to colour	Gene expression pattern
carns1	carnosine synthase 1	Purine binding	orange and blue > yellow and grey
mcm6	minichromosome maintenance protein 6	Purine binding	orange and blue > yellow and grey
myh7	myosin heavy chain 7	Purine metabolism	orange and blue > yellow and grey
nt5c1a	5′-nucleotidase cytosolic IA	Purine metabolism	orange and blue > yellow and grey
ak5	adenylate kinase 5	Purine metabolism	orange and yellow > blue and grey
gne	glucosamine-2-epimerase/N-acetylmannosamine kinase	Purine binding	orange and yellow > blue and grey
itm2c	integral membrane protein 2C	Purine binding	orange and yellow > blue and grey
aldh1a3	aldehyde dehydrogenase 1 family member A3	Carotenoid metabolism	highest in yellow
bcmo1	beta-carotene 1515′-monooxygenase 1	Carotenoid metabolism	highest in yellow
scarb1	scavenger receptor class B member 1	Carotenoid metabolism	highest in yellow
sepp1b	selenoprotein P plasma 1b	–	orange and yellow > grey
adamts13	a disintegrin and metalloproteinase with thrombospondin motifs 13 isoform 1 preproprotein	Iridophore	highest in yellow
anxa1	annexin A1	Iridophore	highest in yellow
bpi	bactericidal/permeability-increasing protein	Iridophore	highest in yellow
phyhd1	phytanoyl-CoA dioxygenase domain containing 1	Iridophore	highest in yellow
sesn1	sestrin 1	Iridophore	highest in yellow
tmem179b	transmembrane protein 179B	Iridophore	highest in yellow
eno3	enolase 3	Iridophore, Purine	lowest in yellow
gnat2	guanine nucleotide binding protein alpha transducing activity polypeptide 2	Iridophore, Purine binding	highest in blue
pald1	phosphatase domain containing paladin 1	Iridophore	highest in blue
fhl2	four and a half LIM domains 2	Iridophore	lowest in blue
dct	dopachrome tautomerase	Melanin pathway	only consistently expressed in grey
tyrp1	tyrosinase-related protein 1	Melanin pathway	highest in grey
oca2	oculocutaneous albinism II	Melanin pathway	highest in grey
slc24a5	solute carrier family 24 member 5	Melanin pathway	highest in grey
slc52a2	solute carrier family 52 member 2	Melanosome biogenesis	highest in grey
rgr	retinal G protein coupled receptor	Melanophore	highest in grey
cndp1	carnosine dipeptidase 1	Melanophore	highest in grey
hpx	hemopexin	Melanin, Tyrosine regulation	grey and blue > orange and yellow
wnt5a	wingless-type MMTV integration site family member 5A	WNT pathway	lowest in yellow
wnt7b	wingless-type MMTV integration site family member 7B	WNT pathway	lowest in yellow
wnt8a	wingless-type MMTV integration site family member 8A	WNT pathway	lowest in yellow
fzd6	frizzled family receptor 6	WNT pathway	highest in blue
dusp2	dual specificity phosphatase 2	Ras/MAPK pathway	grey and blue > orange and yellow
dusp5	dual specificity phosphatase 5	Ras/MAPK pathway	grey and blue > orange and yellow
dusp13	dual specificity phosphatase 13	Ras/MAPK pathway	grey and blue > orange and yellow
dusp14	dual specificity phosphatase 14	Ras/MAPK pathway	grey and blue > orange and yellow
fos	FBJ murine osteosarcoma viral oncogene homolog	Ras/MAPK pathway	highest in blue
fosb	FBJ murine osteosarcoma viral oncogene homolog B	Ras/MAPK pathway	highest in blue
juna	jun B proto-oncogene A	Ras/MAPK pathway	highest in blue
cyp3a4	cytochrome P450 family 3 subfamily A polypeptide 4	Steroid hormone	highest in yellow
cyp3a7	cytochrome P450 family 3 subfamily A polypeptide 7	Steroid hormone	highest in yellow
hsd17b2	hydroxysteroid (17-beta) dehydrogenase 2	Steroid hormone	highest in yellow
scnn1b	sodium channel nonvoltage-gated 1 beta	Steroid hormone	highest in yellow
srd5a2	steroid-5-alpha-reductase alpha polypeptide 2	Steroid hormone	highest in yellow
sult2b1	sulfotransferase family cytosolic 2B member 1	Steroid hormone	highest in blue

Refer to supplementary table S3, Supplementary Material online for further details and additional differentially expressed genes.

Of these, *slc52a2*, *rgr*, and *cndp1* had high expression in grey skin, and *hpx* had high expression in grey and blue skin. Additionally, three genes involved in the WNT signaling pathway (*wnt5a*, *wnt7b*, and *wnt8a*), which indirectly influences melanin synthesis, had higher expression levels in blue, grey and orange skin than in yellow skin, and one gene (*fzd6*) was significantly more highly expressed in blue skin than all other skin colors. We also found that 20 differentially expressed genes included "tyrosine" (the precursor to melanin) in their annotation terms. Notably, these incorporated genes associated with the Ras/MAPK signaling pathway, which like the WNT signaling pathway, indirectly influences melanin synthesis. These genes include: *dusp2*, *dusp5*, *dusp13*, and *dusp14* which all have the highest expression in grey and blue skin, and *fos*, *fosb*, and *juna* which together form the fos/jun transcription factor and are uniquely highly expressed in blue skin (table 2).

Hormone Associated Genes

Abundant evidence indicates control of sex-limited color expression by steroid hormones (Cooper and Greenberg 1992), including in lizards (Cox et al. 2005, 2008; Jessop et al. 2009),

and in *C. decresii* females treated with testosterone express male specific throat coloration (Rankin and Stuart-Fox 2015). We identified six differentially expressed genes associated with steroid hormone pathways: *cyp3a4*, *cyp3a7*, *hsd17b2*, *scnn1b*, and *srd5a2*, all of which were more highly expressed in yellow skin, and *sult2b1* which was highest in blue skin (table 2; supplementary table S3, Supplementary Material online). Differential expression of these genes supports a role for steroid hormones in mediating color expression in *C. decresii*.

Conclusions

By combining metabolomic and transcriptomic analyses of *C. decresii* skin samples, our study contributes substantially to our understanding of the diverse mechanisms of color production in reptiles. We confirmed that yellow or orange skin color is produced by the relative concentration of carotenoid and pteridine pigments, with carotenoid levels highest in yellow skin, and pteridine levels highest in orange skin. The specific metabolites we identified include the vitamin A precursors β-carotene and β-cryptoxanthin, and several genes associated with provitamin A carotenoid metabolism were upregulated in yellow skin. Notably, these metabolites may provide a physiological link between color expression and individual condition (Hill and Johnson 2012). Carotenoid concentrations in the skin may be influenced by environmental availability of carotenoids, which, in turn, may affect pteridine production if individuals maintain a given ratio of specific pigments to produce the desired hue. This is the case in guppies, in which environmental variation in carotenoid availability is correlated with genetically based differences among populations in drosopterin production (Grether et al. 1999, 2005). Thus, identification of genes and pigments associated with skin color in *C. decresii* provides the necessary basis to further explore costs and control of color variation within and between populations.

We have also highlighted 489 genes exhibiting differential expression associated with skin color, including: genes that may be specifically involved in pteridine production in the skin, several genes associated with provitamin A carotenoid metabolism, genes previously associated with iridophore and melanophore cells in zebrafish, genes involved in melanin synthesis and six genes associated with steroid hormone pathways. Nevertheless, the great majority of these 489 genes have not previously been associated with color production in vertebrates and warrant further investigation to confirm their role. These genes also provide a starting point for identifying genes or gene regions associated with color polymorphism in *C. decresii*. In the ruff, *P. pugnax*, the gene *mc1r*, which initiates the production of eumelanin, is located within the large inversion underpinning alternative male reproductive strategies, and exhibits a number of genetic variants associated with the morph types (Lamichhaney et al. 2016). Similarly, it is possible that specific genes responsible for generating skin coloration in *C. decresii* are located within gene regions associated with the discrete throat color polymorphism. More generally, these 489 genes provide a rich resource for investigating the genetic basis of color variation in vertebrates.

Materials and Methods

Study Species and Sample Collection

The lizards used in this study were either wild caught between December 2012 and December 2014 from various locations in South Australia, or bred in captivity between November 2012 and January 2013 to parents from Warren Gorge (31.422°S, 138.705°E; supplementary table S4, Supplementary Material online). Twenty-one adult males were humanely euthanized with an intraperitoneal injection of sodium pentabarbitone (150 mg/kg), and tissues were immediately dissected postmortem. Skin samples for LC-MS analysis were flash-frozen and stored at −80 °C, while tissues for transcriptomic analysis were stored in RNAlater (Ambion, Inc. Austin, TX) at −20 °C. Skin was sampled from a variety of body regions from males of different color morphs (supplementary table S4, Supplementary Material online) to ensure that differences in gene expression were due to skin color rather than morph type or lineage.

Pteridine and Carotenoid Pigment Identification

To determine whether carotenoid or pteridine pigments generate yellow and orange coloration in *C. decresii*, we extracted pigments from seven samples of each of orange, yellow, and grey skin, which incorporated the full throat color variation of the polymorphic northern lineage (fig. 1; Teasdale et al. 2013). A custom pigment extraction was developed for this study and detailed methods are provided in the Supplementary Information (supplementary appendix S1, Supplementary Material online). Briefly, samples were weighed and homogenized in methanol:ethylacetate using a TissueLyser II system (with 3 mm stainless steel beads; Qiagen, Hilden, Germany), and the resulting carotenoid extract was collected following centrifugation. Pteridines were then extracted from the tissue pellet using 2% ammonium hydroxide. Carotenoids and pteridines were semi-quantified in separate LC-MS analyses on an Agilent 6490 triple quadrupole MS system with a Jet Stream electrospray ionization source coupled to an Agilent 1290 series LC system (Agilent Technologies Inc, Santa Clara, CA). Data analysis was conducted using the Agilent MassHunter Workstation Software (version B.07.00). All peak assignments were matched against commercial or purified standards and confirmed with a qualifier ion. Carotenoid standards used were: canthaxanthin, β-carotene, β-cryptoxanthin (Sigma-Aldrich, St Louis, MO), 3′-dehydrolutein, astaxanthin, lutein, and zeaxanthin (these last two isomers cannot be distinguished by this method; Sapphire Biosciences, Redfern, Australia); while pteridine standards were: xanthopterin (Chem-Supply, Port Adelaide, Australia), isoxanthopterin, pterin, pterine-6-carboxylic acid, 6-biopterin (Sigma-Aldrich), sepiapterin (Sapphire Biosciences), and drosopterin (extracted and purified from fruit flies, *Drosophila melanogaster*; Wilson and Jacobson 1977). For each pigment, weight standardized responses were compared among skin colors using one-way ANOVAs and Tukey's *post hoc* tests performed in the stats R package (R Development Core

Team 2010). Data were log transformed prior to analysis to meet model assumptions of normality.

Transcriptome Sequencing, Filtering, and Assembly

RNA was extracted from three blue skin, four orange skin, two yellow skin, four grey skin, and nine nonskin (one of each of heart, pituitary, and thymus and two of each of gonad, retina, and spleen) tissue samples. We used a TissueLyser II system (with 5mm stainless steel beads; Qiagen, Hilden, Germany) to disrupt and homogenize samples before extracting total RNA using an RNeasy Mini Kit (Qiagen, Hilden, Germany). Library preparation and transcriptome sequencing were done by the Georgia Genomics Facility (GGF; Athens, GA) and the Australian Genomic Research Facility (AGRF; Melbourne, Australia). RNA libraries were prepared using a TruSeq RNA Sample Prep Kit (Illumina, Inc., San Diego, CA), including a step for polyA enrichment of messenger RNA (mRNA). Libraries were checked for quality with Bioanalyzer (Agilent Technologies, Inc., Clara, CA) runs and 150 base paired end reads (insert size 250 bp) were then sequenced on the HiSeq2000 sequencing platform (Illumina, Inc., San Diego, CA). Samples were multiplexed with two, six, or twelve libraries sequenced on a single lane, generating between 12.4 and 51.5 M paired end reads per sample (supplementary table S5, Supplementary Material online).

We assessed the quality of the raw reads using FastQC ver. 0.11.2 (Andrews 2010). Adaptor sequences and low quality reads were removed using Trimmomatic ver. 0.32 (Bolger et al. 2014), with a minimum quality (Phred) score of 20 per 8 bp sliding window and a minimum sequence length of 40 bp. Additionally, we used Deconseq ver. 0.4.3 (Schmieder and Edwards 2011) to remove potential contaminant reads. Custom contaminant databases were prepared using the Genome Reference Consortium human genome assembly (GRCh38), and all available bacterial and viral genomic sequences, as downloaded from the National Centre for Biotechnology Information (NCBI) on April 2, 2015. To prepare the rRNA and mitochondrial Deconseq databases, we first *de novo* assembled the trimmed and filtered reads for one transcriptome (49_spleen; supplementary table S6, Supplementary Material online) using Trinity ver. 2.0.6 (Grabherr et al. 2011; Haas et al. 2013) with default settings and a minimum contig length of 151 bp. We then downloaded all available mitochondrial sequences for the family Agamidae, and 18S and 28S rRNA sequences for the suborder Iguania from the NCBI protein database. The assembled transcriptome was compared to these sequences using the BlastN algorithm (with a minimum *E*-value threshold of 10-10; Altschul et al. 1990) to identify the full mitochondrial and rRNA sequences. Deconseq was run using threshold values of $\geq$90% sequence coverage and $\geq$95% sequence identity. For a detailed summary of trimming and filtering statistics refer to supplementary table S5, Supplementary Material online. Assemblies were then constructed from the trimmed and filtered reads for each transcriptome using the program Trinity ver. 2.0.6 (Grabherr et al. 2011; Haas et al. 2013) with default settings and a minimum contig length of 151 bp (supplementary table S6, Supplementary Material online), and assessed for completeness using BUSCO (Benchmarking Universal Single-Copy Orthologs) ver. 1.1b (Simão et al. 2015) and the vertebrata library consisting of 3023 single copy orthologs. Based on this assessment, the average completeness of transcriptome assemblies was 64.9% ($\pm$ 9.6), with 8.9% ($\pm$ 2.2) fragmented, and 26.2% ($\pm$ 7.5) missing BUSCOs (supplementary table S7, Supplementary Material online).

Abundance Estimation and Differential Expression of Genes and Pathways

The central bearded dragon (*Pogona vitticeps*) is currently the closest con-familial species for which a fully annotated genome is available (Georges et al. 2015). Nevertheless, estimated divergence between *C. decresii* and *P. vitticeps* is considerable (Hugall et al. 2008), hence we derived a *C. decresii* specific reference by identifying homologs to the 19,407 protein coding regions annotated for *P. vitticeps*. This was achieved by pooling and comparing the 22 assemblies to the *P. vitticeps* proteome set using blastx. After merging redundant transcripts, correcting frameshifts and removing the untranslated regions, the final *C. decresii* reference used for downstream mapping comprised 17,216 coding DNA sequences. We identified genes within the reference which have been previously shown to be associated with chromatophore cells (Higdon et al. 2013), melanin, and pteridine pigment synthesis pathways (Braasch et al. 2007; Emaresi et al. 2013; Roulin and Ducrest 2013) and/or carotenoid pigment transport and storage (Diepeveen and Salzburger 2001; Salzburger et al. 2007; von Lintig 2010; Walsh et al. 2011) in fish and birds (as there were heretofore no data for nonavian reptiles). We also downloaded Gene Ontology (GO) terms and Kyoto Encyclopedia of Genes and Genomes (KEGG) pathway information for any genes which were differentially expressed between skin colors and searched for key words relating to pigments and pigment precursors (purine, tyrosine, melanin, melanogenesis, pteridine, and carotenoid).

We calculated relative expression levels of genes (in transcripts per million reads; TPM) by mapping the trimmed and filtered reads for each transcriptome to the reference using RSEM (Li and Dewey 2011) and Bowtie 2 v2.2.2 (Langmead and Salzberg 2012). Differentially expressed genes were identified using the Bioconductor package edgeR (Robinson et al. 2010). We first filtered the data so that only those genes with at least one count per million reads in at least two libraries (minimum number of replicates for a skin color) were retained for the analysis and applied trimmed mean of M-values (TMM) normalization (Robinson and Oshlack 2010). Dispersion was estimated on a tag wise basis and *P*-values were adjusted using the false discovery rate (FDR) correction method (Benjamini and Hochberg 1995). To minimize the influence of outlier expression estimates on *P*-values, we adjusted prior.df so that prior.n was equal to one for each comparison. Genes were considered to be significantly differentially expressed when the FDR corrected *P*-value was less than 0.05 and expression values did not overlap between the two groups compared. To further examine clustering of tissue types and skin colors, we performed two principal components analyses (PCAs) using the FactoMineR package

in R (Lê et al. 2008). The first analysis incorporated all samples and all 17,216 annotated genes, while the second analysis incorporated skin samples and the subset of genes which were differentially expressed between skin colors.

We also applied GSEA (ver. 2.0; Subramanian et al. 2005) to expression data to investigate whether pigment related pathways were differentially expressed between skin colors. We produced three custom gene sets for the analysis: (1) "pteridine synthesis" which consisted of the 10 genes listed in the pteridine synthesis pathway in figure 3, (2) "carotenoid metabolism" which consisted of 39 genes involved in provitamin A carotenoid transport and metabolism (Waagmeester et al. 2009), and (3) "melanin synthesis" which incorporated the 81 genes in the KEGG melanogenesis pathway (acs04916; supplementary table S8, Supplementary Material online). We considered pathways to be enriched in one skin color over another when the FDR corrected *P*-value was less than 0.05.

Availability of Data and Materials

The datasets used and/or analyzed during the current study are available from Dryad: doi:10.5061/dryad.ns315.

Supplementary Material

Supplementary data are available at *Molecular Biology and Evolution* online.

Authors' Contributions

CM, AM, and DSF designed the research. CM, AM, and DSF performed the fieldwork. CM and AM performed the transcriptomic analysis. AL and KR performed the metabolomic analysis. CM analyzed and interpreted the data. CM wrote the manuscript. AL, KR, AM, and DSF edited the manuscript. All authors read and approved the final manuscript.

Acknowledgments

We are grateful to Adam Elliott, Jessica Hacking, Anna Lewis, Luisa Teasdale and Madeleine Yewers for assistance with field work and sample collection. Metabolite analysis was conducted at Metabolomics Australia (The University of Melbourne), a National Collaborative Research Infrastructure Strategy initiative under Bioplatforms Australia Pty Ltd. Fieldwork was conducted with approval from the South Australia Department of Environment, Water and Natural Resources (permit: E25861-1) and ethics approvals for all procedures were obtained from the South Australian Wildlife Ethics Committee (18/2010) and The University of Melbourne Animal Ethics Committee (1011760.1). This work was supported by the Australian Research Council (DP150101044) to DSF, and The University of Melbourne, Alfred Nicholas Fellowship to CM.

References

Alonso S, Izagirre N, Smith-Zubiaga I, Gardeazabal J, Díaz-Ramón JL, Díaz-Pérez JL, Zelenika D, Boyano MD, de la Rúa C. 2008. Complex signatures of selection for the melanogenic loci TYR, TYRP1 and DCT in humans. *BMC Evol Biol*. 8:74.

Altschul SF, Gish W, Miller W, Myers EW, Lipman DJ. 1990. Basic local alignment search tool. *J Mol Biol*. 215:403–410.

Andrews S. 2010. FastQC: A quality control tool for high throughput sequence data [Internet]. Available from: http://www.bioinformatics.babraham.ac.uk/projects/fastqc/.

Bagnara JT, Fernandez PJ, Fujii R. 2007. On the blue coloration of vertebrates. *Pigment Cell Res*. 20:14–26.

Benjamini Y, Hochberg Y. 1995. Controlling the false discovery rate: a practical and powerful approach to multiple testing. *J R Stat Soc Series B Stat Methodol*. 57:289–300.

Bolger AM, Lohse M, Usadel B. 2014. Trimmomatic: a flexible trimmer for Illumina sequence data. *Bioinformatics* 30:2114–2120.

Braasch I, Schartl M, Volff J-N. 2007. Evolution of pigment synthesis pathways by gene and genome duplication in fish. *BMC Evol Biol*. 7:74.

Cooper WE, Greenberg N. 1992. Reptilian coloration and behavior. In: Gans C, Crews D, editors. Biology of the reptilia, volume 18: hormones, brain, and behavior. Chicago: University of Chicago Press.

Cox RM, Skelley SL, Leo A, John-Alder HB. 2005. Testosterone regulates sexually dimorphic coloration in the eastern fence lizard, *Sceloporus undulatus*. *Copeia* 2005:597–608.

Cox RM, Zilberman V, John-Alder HB. 2008. Testosterone stimulates the expression of a social color signal in Yarrow's Spiny Lizard, *Sceloporus jarrovii*. *J Exp Zool A Ecol Genet Physiol*. 309A:505–514.

Diepeveen ET, Salzburger W. 2001. Molecular characterization of two endothelin pathways in East African cichlid fishes. *J Mol Evol*. 73:355–368.

Emaresi G, Ducrest A-L, Bize P, Richter H, Simon C, Roulin A. 2013. Pleiotropy in the melanocortin system: expression levels of this system are associated with melanogenesis and pigmentation in the tawny owl (*Strix aluco*). *Mol Ecol*. 22:4915–4930.

Eroglu A, Harrison EH. 2013. Carotenoid metabolism in mammals, including man: formation, occurrence, and function of apocarotenoids. *J Lipid Res*. 54:1719–1730.

Fitze PS, Cote J, San-Jose LM, Meylan S, Isaksson C, Andersson S, Rossi J-M, Clobert J. 2009. Carotenoid-based colours reflect the stress response in the common lizard. *PLoS One* 4:e5111.

Georges A, Li Q, Lian J, O'Meally D, Deakin J, Wang Z, Zhang P, Fujita M, Patel HR, Holleley CE, et al. 2015. High-coverage sequencing and annotated assembly of the genome of the Australian dragon lizard *Pogona vitticeps*. *GigaScience* 4:45.

Gibbons JRH. 1979. The hind leg pushup display of the *Amphibolurus decresii* species complex (Lacertilia: Agamidae). *Copeia* 1979:29–40.

Grabherr MG, Haas BJ, Yassour M, Levin JZ, Thompson DA, Amit I, Adiconis X, Fan L, Raychowdhury R, Zeng Q. 2011. Full-length transcriptome assembly from RNA-Seq data without a reference genome. *Nat Biotechnol*. 29:644–652.

Grether GF, Cummings ME, Hudon J. 2005. Countergradient variation in the sexual coloration of guppies (*Poecilia reticulata*): Drosopterin synthesis balances carotenoid availability. *Evolution* 59:175–188.

Grether GF, Hudon J, Millie DF. 1999. Carotenoid limitation of sexual coloration along an environmental gradient in guppies. *Proc R Soc Lond B Biol Sci*. 266:1317–1322.

Grether GF, Kollura GR, Nersissian K. 2004. Individual colour patches as multi-component signals. *Biol Rev*. 79:583–610.

Haas BJ, Papanicolaou A, Yassour M, Grabherr M, Blood PD, Bowden J, Couger MB, Eccles D, Li B, Lieber M. 2013. De novo transcript sequence reconstruction from RNA-seq using the Trinity platform for reference generation and analysis. *Nat Protoc*. 8:1494–1512.

Haisten DC, Paranjpe D, Loveridge S, Sinervo B. 2015. The cellular basis of polymorphic coloration in common side-blotched lizards, *Uta stansburiana*. *Herpetologica* 71:125–135.

Higdon CW, Mitra RD, Johnson SL. 2013. Gene expression analysis of zebrafish melanocytes, iridophores and retinal pigmented epithelium reveals indicators of biological function and developmental origin. *PLoS One* 8:e67801.

Hill GE, Johnson JD. 2012. The vitamin A–redox hypothesis: a biochemical basis for honest signalling via carotenoid pigmentation. *Am Nat*. 180:E127–E150.

Hoekstra HE. 2006. Genetics, development and evolution of adaptive pigmentation in vertebrates. *Heredity* 97:222–234.
Houston TF, Hutchinson M. 1998. Dragon lizards and goannas of South Australia. Adelaide: South Australian Museum.
Hubbard JK, Uy AC, Hauber ME, Hoekstra HE, Safran RJ. 2010. Vertebrate pigmentation: from underlying genes to adaptive function. *Trends Genet*. 26:231–239.
Hugall AF, Foster R, Hutchinson M, Lee MSY. 2008. Phylogeny of Australasian agamid lizards based on nuclear and mitochondrial genes: implications for morphological evolution and biogeography. *Biol J Linn Soc Lond*. 93:343–358.
Jessop TS, Chan R, Stuart-Fox D. 2009. Sex steroid correlates of female-specific colouration, behaviour and reproductive state in Lake Eyre dragon lizards, *Ctenophorus maculosus*. *J Comp Physiol A Neuroethol Sens Neural Behav Physiol*. 195:619–630.
Küpper C, Stocks M, Risse JE, dos Remedios N, Farrell LL, McRae SB, Morgan TC, Karlionova N, Pinchuk P, Verkuil YI, et al. 2016. A supergene determines highly divergent male reproductive morphs in the ruff. *Nat Genet*. 48:79–86.
Lamason RL, Mohideen MA, Mest JR, Wong AC, Norton HL, Aros MC, Jurynec MJ, Mao X, Humphreville VR, Humbert JE, et al. 2005. SLC24A5, a putative cation exchanger, affects pigmentation in zebrafish and humans. *Science* 310:1782–1786.
Lamichhaney S, Fan G, Widemo F, Gunnarsson U, Schwoshow Thalmann D, Hoeppner MP, Kerje S, Gustafson U, Shi C, Zhang H, et al. 2016. Structural genomic changes underlie alternative reproductive strategies in the ruff (*Philomachus pugnax*). *Nat Genet*. 48:84–90.
Langmead B, Salzberg SL. 2012. Fast gapped-read alignment with Bowtie 2. *Nat Methods* 9:357–359.
Lê S, Josse J, Husson F. 2008. FactoMineR: an R package for multivariate analysis. *J Stat Softw*. 25: 18.
Li B, Dewey CN. 2011. RSEM: accurate transcript quantification from RNA-Seq data with or without a reference genome. *BMC Bioinformatics* 12:323.
Lopes RJ, Johnson JD, Toomey MB, Ferreira MS, Araujo PM, Melo-Ferreira J, Andersson L, Hill GE, Corbo JC, Carneiro M. 2016. Genetic basis for red coloration in birds. *Curr Biol*. 26:8–1.
Macedonia JM, James S, Wittle LW, Clark DL. 2000. Skin pigments and coloration in the Jamaican radiation of *Anolis* lizards. *J Herp*. 34:99–109.
McGraw KJ. 2006. Mechanisms of carotenoid-based coloration. In: Hill GE, McGraw KJ, editors. Bird coloration: mechanisms and measurements. Cambridge (MA): Harvard University Press.
McLean CA, Moussalli A, Sass S, Stuart-Fox D. 2013. Taxonomic assessment of the *Ctenophorus decresii* (Reptilia: Agamidae) complex reveals a new species of dragon lizard from western New South Wales. *Rec Aus Mus*. 65:51–63.
McLean CA, Moussalli A, Stuart-Fox D. 2014a. Local adaptation and divergence in colour signal conspicuousness between monomorphic and polymorphic lineages in a lizard. *J Evol Biol*. 27:2654–2664.
McLean CA, Stuart-Fox D, Moussalli A. 2014b. Phylogeographic structure, demographic history and morph composition in a colour polymorphic lizard. *J Evol Biol*. 27:2123–2137.
Merkling T, Hamilton DG, Cser B, Svedin N, Pryke SR. 2015. Proximate mechanisms of colour variation in the frillneck lizard: geographical differences in pigment contents of an ornament. *Biol J Linn Soc Lond*. 117:503–515.
Morrison RL, Rand MS, Frostmason SK. 1995. Cellular basis of color differences in 3 morphs of the lizard *Sceloporus undulatus erythrocheilus*. *Copeia* 1995:397–408.
Mundy NI, Stapley J, Bennison C, Tucker R, Twyman H, Kim K-W, Burke T, Birkhead TR, Andersson S, Slate J. 2016. Red carotenoid coloration in the zebra finch is controlled by a cytochrome P450 gene cluster. *Curr Biol*. 26:1435–1440.
Olson VA, Owens IPF. 1998. Costly sexual signals: are carotenoids rare, risky or required? *Trends Ecol Evol*. 13:510–514.
Olsson M, Stuart-Fox D, Ballen C. 2013. Genetics and evolution of colour patterns in reptiles. *Semin Cell Dev Biol*. 24:529–541.
Olsson M, Wilson M, Isaksson C, Uller T, Mott B. 2008. Carotenoid intake does not mediate a relationship between reactive oxygen species and bright colouration: experimental test in a lizard. *J Exp Biol*. 211:1257–1261.
Poelstra JW, Vijay N, Hoeppner MP, Wolf JBW. 2015. Transcriptomics of colour patterning and coloration shifts in crows. *Mol Ecol*. 24:4617–4628.
R Development Core Team. 2010. R: A language and environment for statistical computing. R Foundation for Statistical Computing, Vienna, Austria. Available from: http://www.R-project.org/.
Rankin K, Stuart-Fox D. 2015. Testosterone-induced expression of male colour morphs in females of the polymorphic tawny dragon lizard, *Ctenophorus decresii*. *PLoS One* 10:e0140458.
Rankin KJ, McLean CA, Kemp DJ, Stuart-Fox D. 2016. The genetic basis of discrete and quantitative colour variation in the polymorphic lizard, *Ctenophorus decresii*. *BMC Evol Biol*. 16:179.
Robinson MD, McCarthy DJ, Smyth GK. 2010. EdgeR: a Bioconductor package for differential expression analysis of digital gene expression data. *Bioinformatics* 26:139–140.
Robinson MD, Oshlack A. 2010. A scaling normalization method for differential expression analysis of RNA-seq data. *Genome Biol*. 11:R25.
Roulin A, Ducrest A-L. 2013. Genetics of colouration in birds. *Semin Cell Dev Biol*. 24:594–608.
Saenko SV, Yeyssier J, van der Marel D, Milinkovitch MC. 2013. Precise colocalization of interacting structural and pigmentary elements generates extensive color pattern variation in *Phelsuma* lizards. *BMC Biol*. 11:105.
Salzburger W, Braasch I, Meyer A. 2007. Adaptive sequence evolution in a colour gene involved in the formation of the characteristic egg-dummies of male haplochromine cichlid fishes. *BMC Biol*. 5:51.
Sams CE, Panthee DR, Charron CS, Kopsell DA, Yuan JS. 2011. Selenium regulates gene expression for glucosinolate and carotenoid biosynthesis in Arabidopsis. *J Am Soc Hortic Sci*. 136:23–34.
Schmieder R, Edwards R. 2011. Fast identification and removal of sequence contamination from genomic and metagenomic datasets. *PLoS One* 6:e17288.
Schweizer RM, Robinson J, Harrigan R, Silva P, Galverni M, Musiani M, Green RE, Novembre J, Wayne RK. 2016. Targeted capture and resequencing of 1040 genes reveal environmentally driven functional variation in grey wolves. *Mol Ecol*. 25:357–379.
Simão FA, Waterhouse RM, Ioannidis P, Kriventseva EV, Zdobnov EM. 2015. BUSCO: assessing genome assembly and annotation completeness with single-copy orthologs. *Bioinformatics* 31:3210–3212.
Steffen JE, Hill GE, Guyer C. 2010. Carotenoid access, nutritional stress, and the dewlap color of male brown anoles. *Copeia* 2010:239–246.
Steffen JE, McGraw KJ. 2009. How dewlap color reflects its carotenoid and pterin content in male and female brown anoles (*Norops sagrei*). *Comp Biochem Physiol Biochem Mol Biol*. 154:334–340.
Subramanian A, Tamayo P, Mootha VK, Mukherjee S, Ebert BL, Gillette MA, Paulovich A, Pomeroy SL, Golub TR, Lander ES, et al. 2005. Gene set enrichment analysis: a knowledge-based approach for interpreting genome-wide expression profiles. *Proc Natl Acad Sci U S A*. 102:15545–15550.
Svensson PA, Wong BBM. 2011. Carotenoid-based signals in behavioural ecology: a review. *Behaviour* 148:131–189.
Teasdale LC, Stevens M, Stuart-Fox D. 2013. Discrete colour polymorphism in the tawny dragon lizard (*Ctenophorus decresii*) and differences in signal conspicuousness among morphs. *J Evol Biol*. 26:1035–1046.
Toews DPL, Taylor SA, Vallender R, Brelsford A, Burtcher BG, Messer PW, Lovette IJ. 2016. Plumage genes and little else distinguish the genomes of hybridizing warblers. *Curr Biol*. 26:2313–2318.
Tuttle EM, Bergland AO, Korody ML, Brewer MS, Newhouse DJ, Minx P, Stager M, Betuel A, Cheviron ZA, Warren WC, et al. 2016. Divergence and functional degradation of a sex chromosome-like supergene. *Curr Biol*. 26:344–350.

von Lintig J. 2010. Colors with functions: elucidating the biochemical and molecular basis of carotenoid metabolism. *Annu Rev Nutr*. 30:35–56.

Waagmeester A, Pezik P, Coort S, Tourniaire F, Evelo C, Rebholz-Schuhmann D. 2009. Pathway enrichment based on text mining and its validation on carotenoid and vitamin A metabolism. *Omics* 13:367–379.

Walsh N, Dale J, McGraw KJ, Pointer MA, Mundy NI. 2011. Candidate genes for carotenoid coloration in vertebrates and their expression profiled in the carotenoid-containing plumage and bill of a wild bird. *Proc R Soc Lond B Biol Sci*. 279:58–66.

Weiss SL, Foerster K, Hudon J. 2012. Pteridine, not carotenoid, pigments underlie the female-specific orange ornament of striped plateau lizards (*Sceloporus virgatus*). *Comp Biochem Physiol*. 161:117–123.

Wilson TG, Jacobson KB. 1977. Isolation and characterization of pteridines from heads of *Drosophila melanogaster* by a modified thin-layer chromatography procedure. *Biochem Genet*. 15:307–319.

Yewers MSC, McLean CA, Moussalli A, Stuart-Fox D, Bennett ATD, Knott B. 2015. Spectral sensitivity of cone photoreceptors and opsin expression in two colour-divergent lineages of the lizard *Ctenophorus decresii*. *J Exp Biol*. 218:1556–1563.

Yewers MSC, Pryke SR, Stuart-Fox D. 2016. Behavioural differences across contexts may indicate morph-specific strategies in the lizard *Ctenophorus decresii*. *Anim Behav*. 111:329–339.

Ziegler I. 2003. The pteridine pathway in zebrafish: regulation anf specification during the determination of neural crest cell-fate. *Pigment Cell Res*. 16:172–182.